ISSN1027-5495. Functional Materials, 32, No.3 (2025), p. 429-440
doi:http://dx.doi.org/10.15407/fm32.03.429 © 2025 — STC "Institute for Single Crystals"

Synthesis and electrophysical properties of fluoride conducting phases $Ba_{1-y-x}La_xSn_{1+y}F_{4+x}$

O.V. Lysenko[1], R.M. Pshenychnyi[2], A.O. Omelchuk[1]

[1]V.I. Vernadsky Institute of General and Inorganic Chemistry, NAS of Ukraine 32-34, Acad. Palladina Ave., 03680 Kyiv, Ukraine
[2]Sumy State University 116, Kharkivska st., 40007 Sumy, Ukraine

Received April 22, 2025

In this paper, the electroconductive properties of solid non-stoichiometric phases formed in the BaF_2–LaF_3–SnF_2. The $Ba_{0.86-x}La_xSn_{1.14}F_{4+x}$ and $Ba_{0.8-x}La_xSn_{1.2}F_{4+x}$ phases containing up to 0.12 mole fractions lanthanum were synthesized by the method of co-precipitation of BaF_2 and LaF_3 followed by sintering with SnF_2. The crystal lattice of the synthesized compounds corresponds to the tetragonal syngony (space group *P4/nmm*) and is isostructural to $BaSnF_4$. The electrical conductivity of the synthesized phases depends on the pressure at which the samples were prepared. Samples made at a pressure of 9.8 MPa have the highest conductivity. The electrical conductivity of the synthesized solutions of heterovalent substitution $Ba_{0.86-x}La_xSn_{1.14}F_{4+x}$ and $Ba_{0.8-x}La_xSn_{1.2}F_{4+x}$ is higher than the conductivity of the initial non-stoichiometric phases $Ba_{0.86}Sn_{1.14}F_{4.00}$ and $Ba_{0.80}Sn_{1.20}F_{4.00}$, and the activation energy of electrical conductivity is lower. An increase in the substituent amount: to 0.12 for $Ba_{0.86-x}La_xSn_{1.14}F_{4+x}$ and to 0.10 for $Ba_{0.8-x}La_xSn_{1.2}F_{4+x}$ positively affects the electrical conductivity of the obtained electrolytes. Analysis of the isothermal conductivity surface of the fluoride conducting phases $Ba_{1-y-x}La_xSn_{1+y}F_{4+x}$ $x \le 0.12$, $y \le 0.2$ indicates that the conductivity of solid electrolytes increases with increasing concentration of lanthanum and tin in the material. The electronic component of conductivity for the samples with different cationic composition, and the charge transfer numbers of fluorine anions were estimated. The conductivity of all synthesized phases is determined by fluorine anions, the charge transfer numbers are close to unity.

Key words: fluoride-conducting phases, fluorides of tin, barium, lanthanum, solid substitution solutions, electrical conductivity, X-ray diffraction, voltammetry.

Синтез та електрофізичні властивості фторидпровідних фаз $Ba_{1-y-x}La_xSn_{1+y}F_{4+x}$.
О.В. Лисенко, Р.М. Пшеничний, А.О. Омельчук

Досліджено **електропровідні властивості твердих нестехіометричних фаз, утворених** у системі BaF_2-LaF_3-SnF_2. Методом співосадження BaF_2 і LaF_3 з подальшим спіканням з SnF_2 синтезовано фази $Ba_{0,86-x}La_xSn_{1,14}F_{4+x}$ і $Ba_{0,8-x}La_xSn_{1,2}F_{4+x}$, які містять до 0,12 мольних частин лантану. Кристалічна решітка синтезованих сполук відповідає тетрагональній сингонії (пр. гр. *P4/nmm*) та ізоструктурна $BaSnF_4$. Електропровідність синтезованих фаз залежить від тиску. Найбільшу електропровідність мають зразки, виготовлені під тиском 9,8 МПа. Електропровідність синтезованих розчинів гетеровалентного заміщення $Ba_{0,86-x}La_xSn_{1,14}F_{4+x}$ та $Ba_{0,8-x}La_xSn_{1,2}F_{4+x}$ вища за електропровідність вихідних нестехіометричних фаз $Ba_{0,86}Sn_{1,14}F_{4,00}$ та $Ba_{0,80}Sn_{1,20}F_{4,00}$, а енергія активації електропровідності менша. Встановлено, що збільшення кількості замісника позитивно впливає на електропровідність отриманих електролітів для $Ba_{0,86-x}La_xSn_{1,14}F_{4+x}$ до 0,12 і для $Ba_{0,8-x}La_xSn_{1,2}F_{4+x}$до0,10.Аналізізотермічноїповерхніелектропровідностіфторидпровідних фаз $Ba_{1-y-x}La_xSn_{1+y}F_{4+x}$ **$x \le 0{,}12$, $y \le 0{,}2$ показує, що електропровідність твердих електролітів зростає** зі збільшенням концентрації лантану та стануму в матеріалі. Оцінено електронну складову електропровідності синтезованих зразків різного катіонного складу, розраховано числа переносу заряду аніонами фтору. Електропровідність усіх синтезованих фаз визначається аніонами фтору, числа переносу заряду близькі до одиниці.

1. Introduction

One of the urgent problems of modern science and technology is the growing need for new generation chemical current sources. This is due, on the one hand, to the limited natural resources of raw materials for the manufacture of known commercial current sources, and on the other hand, to the rapid growth in the production of devices for various purposes, that require electrical energy for power supply. It is also necessary to take into account the sharp increase in demand for clean energy, because recently, due to the excessive and irrational use of traditional energy sources, humanity has faced a number of global problems that require urgent solutions. These include air pollution by emissions from industry, internal combustion engines and greenhouse gases, cousing irreversible climate change and limited deposits of natural resources; that is why there is a need to create new energy sources.

Significant progress in solving these problems can be achieved by creating a new generation of energy sources, in which Red/Ox processes occur under the influence of solar radiation, wind and hydropower, and charge transfer occurs in solid ion conducting materials. All-solid-state current sources made from ion conducting materials are expected to have a significantly higher energy density compared to known commercial lithium-ion batteries [1-5]. Solid fluoride conducting phases suitable for the development of new generation current sources have become the object of intensive research [6, 7]. Accumulation of experimental data and generalization of principles for creating such materials is today not only a scientific, but also an applied task of modern electrochemistry.

Currently, the systems with the highest fluorine conductivity include compounds of the composition $MSnF_4$ (where M - Pb, Ba, Sr) and solid solutions based on them [1, 8]. The compound ß-$PbSnF_4$ among the fluorine-conducting phases known today has one of the largest unipolar ionic conductivity at room temperature (RT), which is $1.2 \cdot 10^{-3}$ S/cm [9, 10]. Electrolyte materials based on it are characterized by relatively low decomposition voltages, which limits the use of a number of metals (Mg, Ca, etc.) with a high negative electrode potential for use as anodes in fluoride-ion batteries [11,12]. The creation of electrolytes based on metal fluorides with high Gibbs energy of their formation allows increasing the voltage of their decomposition. In this regard, fluorine-conducting phases formed in the BaF_2-SnF_2 system with additives of rare earth fluorides are attractive [13]. They are characterized by a relatively higher thermodynamic decomposition voltage, although they have a slightly lower ion conductivity. In addition, they do not contain toxic lead compounds.

In the BaF_2-SnF_2 system, with the ratio of the initial components 50/50, a complex fluoride of stoichiometric composition $BaSnF_4$ with the ß-$PbSnF_4$ structure is formed with an electrical conductivity several orders of magnitude higher than individual barium and tin fluorides [13, 14]. In this system, solid solutions $(BaF_2)_x$–$(SnF_2)_{1-x}$ with highly conductive isostructural $BaSnF_4$ are formed [13].

High conductivity of fluoride conducting phases $MSnF_4$ (where M - Pb, Ba, Sr) is due to the specific electronic structure of the Sn^{2+} cation. The presence of a unshared pair of $5s^2$ electrons determines its high stereoactivity and ability to influence the mobility of fluorine anions in the anionic sublattice [15,16]. The layered structure $BaSnF_4$ formed by alternating layers $\cdots$BaBaSnSnBaBa$\cdots$ along the *c* axis, allows fluorine anions to be placed in three positions between the Ba–Sn, Sn–Sn and Ba–Sn layers [17]. In the plane between the Ba–Ba layers, there are inactive anions, therefore, the migration of fluorine anions occurs mainly between the Sn–Sn, Ba–Sn layers or by jumping into the space between Ba–Sn layers [14].

It has been established [13] that in systems based on the BaF_2–SnF_2, a shift of the ratio of components towards increasing the amount of tin (II) fluoride leads to the formation of fluorine-conducting phases with higher conductivity compared to $BaSnF_4$. In addition, heterovalent substitution of a part of barium cations with cations of rare earth elements contributes to increasing the conductivity of such phases due to an increase in the concentration of point defects. Even a small amount of heterovalent substituent leads to an increase in conductivity and a decrease in activation energy [18–21]. Information on the conductivity of some phases formed in this system is given in [13, 22–24]. It is noted that the phase of the $(BaF_2)_{0.47}(SnF_2)_{0.53}$ composition has a fairly high conductivity ($\sigma = 4.1 \cdot 10^{-3}$ S/cm at RT) and a low activation energy (E_a = 17.9 kJ/mol) of ionic conductivity [13].

It should be noted that the electrical conductivity of solid electrolytes depends not only on

their composition and structure, but also on the conditions of sample preparation. Typically, samples of a certain geometric shape are prepared by pressing a finely dispersed powder of the synthesized fluorine-conducting phase. Most often, they are cylinders. It is noted [25,26] that the conductivity of the sample thus prepared depends not only on the size of the initial crystallites, but also on the pressure under which they are made. Currently, information on the influence of the conditions of sample preparation of fluorine-conducting phases is extremely limited. It is known [25] that the pressure under which samples are prepared for measuring conductivity significantly affects the conductivity of such fluorine-conducting phases: $BaSnF_4$, $PbSnF_4$, $Ba_{0.6}La_{0.4}F_{2.0}$, $La_{0.9}Ba_{0.1}F_{2.9}$.

Currently, there are no generally accepted conditions for the manufacture of electrode and electrolyte materials for solid-state current sources, in particular for fluoride electrolyte ones. In this regard, it is important to study and accumulate experimental data not only on methods for selecting components and synthesis of fluorine-conducting phases, but also on the preparation of samples for research and the conditions of their manufacture.

The paper presents the results on the conductivity depending on the composition and conditions for the preparation of samples of the BaF_2–LaF_3–SnF_2 system. The contribution of the electron component to the total conductivity was evaluated and the charge transfer numbers of fluorine anions were calculated for the synthesized samples.

2. Experimental

For the synthesis of solid fluorine-conducting phases, the following reagents were used: La_2O_3 (99%), $Ba(NO_3)_2$ (99.95%), SnF_2 (99%) та NH_4F (99%).

Fluorine-conducting phases were synthesized in several steps [20, 27, 28]. In the first one, solid solutions of $Ba_{1-x}La_xF_{2+x}$, were synthesized by co-precipitation from aqueous-alcoholic solutions. For synthesis, 0.1 M aqueous-alcoholic solutions of $Ba(NO_3)_2$ and $La(NO_3)_3$ were used, and as a precipitant – an aqueous-alcoholic solution NH_4F in a 7-fold excess. The stock solutions were mixed in the calculated ratios and homogenized by magnetic stirring for 10 minutes, then the precipitant solution was added dropwise. The precipitate was washed with distilled water several times and separated by centrifugation, then air-dried for 24 hours at 333 K.

In the second step, the synthesized $Ba_{1-x}La_xF_{2+x}$ phases were sintered with tin (II) fluoride in calculated amounts to produce solid fluorine-conducting phases of the $BaSnF_4$ structure in the BaF_2–LaF_3–SnF_2 system. Sintering was carried out in an argon atmosphere at a temperature of 773 K for 30 minutes. Synthesis of the $Ba_{1-y-x}La_xSn_{1+y}F_{4+x}$ phases in 2 stages allows obtaining samples with significantly lower specific energy and reagent costs and is much simpler compared to direct solid-phase synthesis from individual barium, lanthanum and tin fluorides, which have different melting points.

The synthesized phases were studied by X-ray diffraction (XRD) methods on a DRON-3M diffractometer with CuK_α-radiation in the range of 2θ angles from 10 to 80 degrees with a step of 0.04 degrees and an exposure of 3 s at each point. Processing and analysis of diffraction patterns were performed using Match software, and unit cell volumes were calculated using UnitCell software. To identify the phases obtained, the diffraction patterns were compared with reference samples of the ICDD database.

Electrical conductivity was determined by the alternating current method using a device RCL E-30. All measurements were carried out under the same conditions using a two-electrode circuit with heat-resistant cells in which cylindrical samples of the fluorine-conducting phase, produced by pressing, were placed between polished platinum electrodes. Conductivity was measured at a frequency of 100 kHz in the temperature range of 298–623 K in an argon atmosphere after thermostatting in cooling mode. The measurement error for electrical conductivity did not exceed 4%, and for temperature – 1%. The overall dimensions of the samples were: diameter 8.0 mm, height 1.2–1.6 mm. The samples were prepared by pressing in a mold with a diameter of 8.0 mm under a pressure of 10 MPa for 3 minutes; the thickness of the obtained polycrystalline samples was 1.2–1.6 mm. To study the dependence of the conductivity of the solid electrolyte on the pressure and granulation density, samples were prepared at different pressures in the range from 7.4 to 14.7 MPa. The density of these samples was determined on an OHAUS PX224 balance with an accuracy of 0.1 mg using the OHAUS 83021512 density determination kit, according to the method described in the instructions

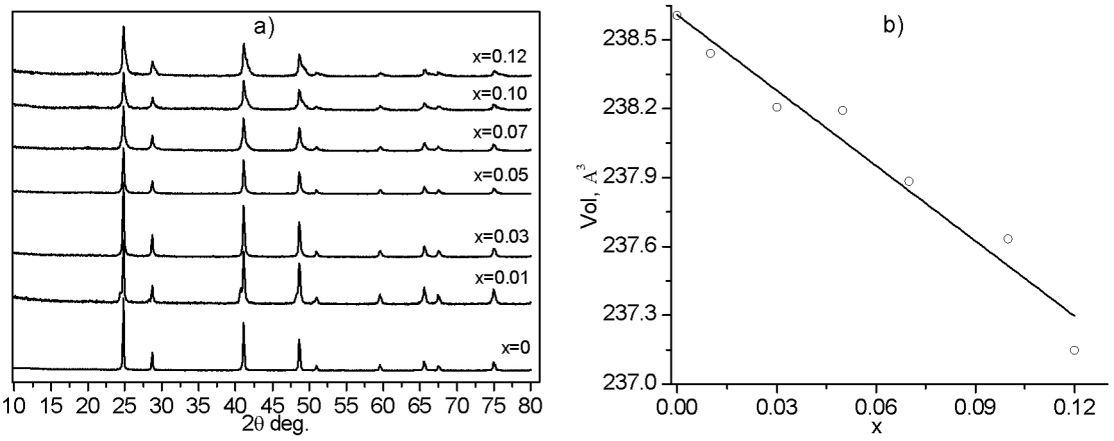

Fig. 1. Diffraction patterns (a) and dependence of unit cell volumes on lanthanum concentration (*x*, mole fractions)" (b) for solid solutions $Ba_{1-x}La_xF_{2+x}$.

for use of this kit. The method of determining density is based on Archimedes' law. This law states that every solid body immersed in a fluid loses weight by an amount equal to that of the fluid it displaces.

The specific conductivity was calculated using the equation:

$$\sigma = l/s \cdot R \qquad (1)$$

where l is the thickness of the cylindrical sample, s is the contact area, R is the active resistance.

The contribution of the electronic component to the total electrical conductivity was determined using the Hebb-Wagner polarization method [29]. The study was carried out using a two-electrode circuit in an electrochemical cell: (–)Ni:NiF_2:CaF_2 | solid-state electrolyte | Pt(+). The composite cathode consisted of a mixture of Ni, NiF_2 and CaF_2 powders in a volume ratio of 3:1:1, respectively. Nickel powder was used as an additive to improve electronic conductivity and calcium fluoride was used to reduce the effect of electrode polarization. The cell with the sample was heated and thermostatted for an hour, then polarized using a laboratory power supply Masteram MR5010E from 0.2V to 3.6V in increments of 0.2V; the current flowing through the cell was recorded using a laboratory multimeter Tektronix DMM4020. For the studies, layer-by-layer compressed samples of solid electrolytes with a composite electrode with a diameter of 8.0 mm and an electrolyte layer thickness of 1.0-1.4 mm were used.

3. Results and discussion

It was established using the X-ray diffraction method, that samples of solid solutions $Ba_{1-x}La_xF_{2+x}$ synthesized at the first stage have a crystal lattice of cubic syngony (space group *Fm3m*), isostructural to barium fluoride (ICDD card No. 00-004-0452 BaF_2) (Fig. 1a). Based on the obtained results, the volumes of sample unit cells were calculated. A linear decrease in the unit cell volume depending on the amount of lanthanum indicates the formation of a substitution solid solution in which part of the Ba^{2+} cations with an effective radius of 0.135 nm is replaced by La^{3+} cations with an effective radius of 0.101 nm (for VI coordination) [30]. This relationship is well consistent with the rules of crystallographic substitution (Fig. 1b).

According to the results of X-ray diffraction, the $Ba_{0.86-x}La_xSn_{1.14}F_{4+x}$ and $Ba_{0.8-x}La_xSn_{1.2}F_{4+x}$ phases have crystalline lattices of tetragonal syngony (space group *P4/nmm*), and are isostructural to $BaSnF_4$ (ICDD card № 00-038-0738 $BaSnF_4$).

The calculated unit cell sizes of the synthesized phases indicate that the substitution of a portion of the Ba^{2+} cations with La^{3+} cations does not significantly affect the unit cell volume. It was found that using the method described above, it is possible to obtain single-phase solid substitution solutions with a maximum content of lanthanum cations of 0.12.

The obtained results indicate that the physicochemical properties of the phases synthesized in this system depend significantly on the pressure at which the samples for measurements are prepared. The dependence of conductivity on pressure during the production of samples of synthesized phases has an extremum. When the pressure increases to certain values, the conductivity of the synthesized phases first increases and then decreases. As the pressure increases, the density of the resulting samples

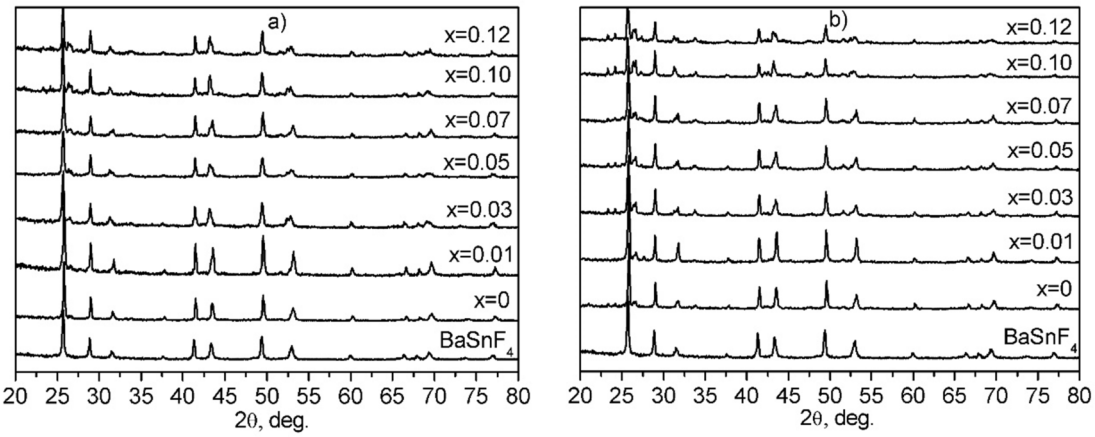

Fig. 2. Diffraction patterns of the obtained phases $Ba_{0.86-x}La_xSn_{1.14}F_{4+x}$ (a) and $Ba_{0.8-x}La_xSn_{1.2}F_{4+x}$ (b).

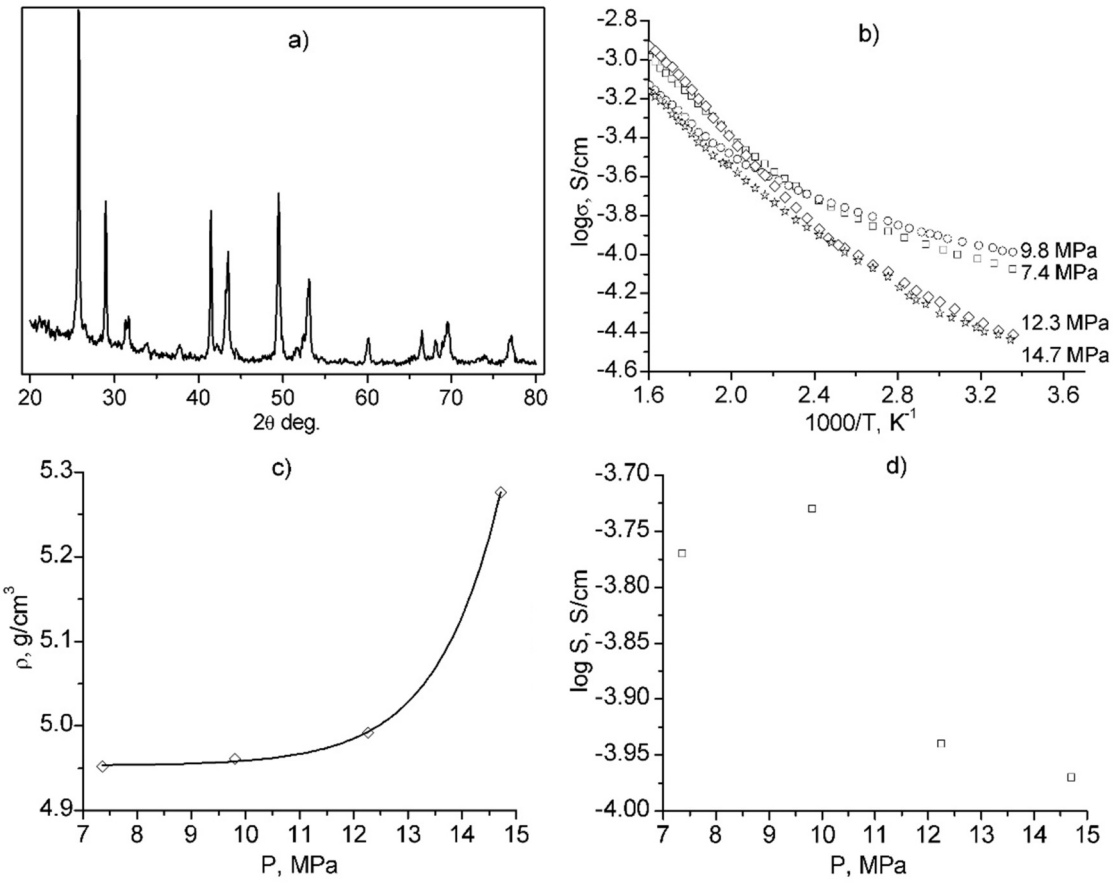

Fig. 3. Diffraction patterns (a) of a sample of the fluorine-conducting phase $Ba_{0.95}La_{0.05}SnF_{4.05}$ and its polyterms of conductivity at different pressures (b), dependence of density on pressure (c) and ion conductivity (d) on pressure at 400 K.

also increases. The typical dependences of conductivity and density of samples on the pressure are shown in Fig. 3 using $Ba_{0.95}La_{0.05}SnF_{4.05}$ as an example. It can be seen that in a certain range of applied pressure, the conductivity initially increases (Fig.3b, 3d) and reaches its maximum value at a pressure of 9.8 MPa in the low-temperature zone; with a further increase in pressure, the conductivity decreases. Density increases exponentially with increasing pressure (Fig. 3c). A similar nature of the dependencies, as noted above, was observed in the study of the properties of solid phases: $BaSnF_4$, $PbSnF_4$, $Ba_{0.6}La_{0.4}F_{2.0}$, $La_{0.9}Ba_{0.1}F_{2.9}$ [25, 26]. The increase in both conductivity and density in a certain range of applied pressures

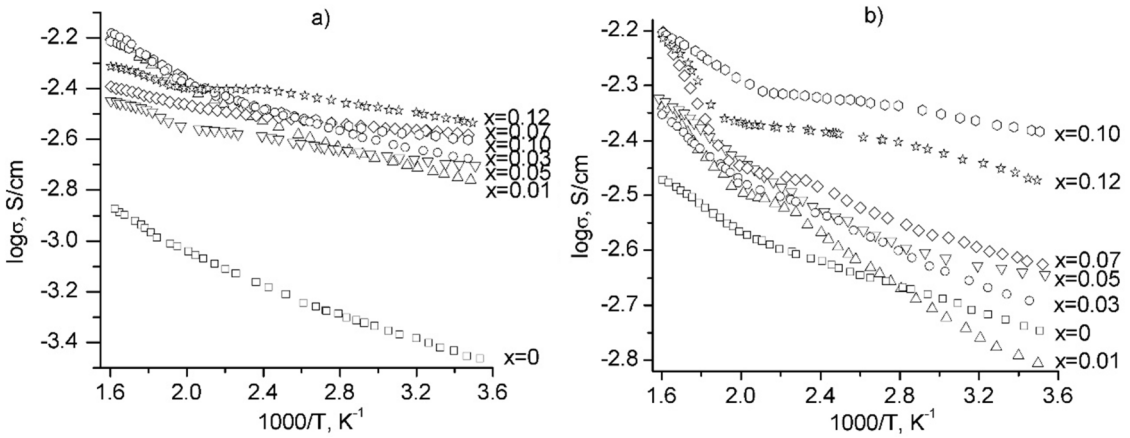

Fig. 4. Temperature dependences of electrical conductivity of fluorine-conducting phase $Ba_{0.86-x}La_xSn_{1.14}F_{4+x}$ (a) and $Ba_{0.8-x}La_xSn_{1.2}F_{4+x}$ (b)

may be because the crystallite size of the synthesized phases initially decreases at the micron and submicron levels, filling the intercrystalline voids, thereby reducing the resistance to charge transfer between them. At higher pressures, deformation of the crystal lattice and a decrease in the size of the unit cell are possible. The density of the sample continues to increase, while the migration of fluoride anions, and therefore the conductivity, decreases. The higher the pressure, the greater the deformation of the unit cell, the lower the mobility of inter-node fluorine anions. Thus, pressure that promotes a reduction in the size of crystallites (compaction) at the micron and submicron levels promotes an increase in conductivity, and pressure that causes deformation of the crystal lattice promotes its decrease. The conductivity isotherms (Fig. 4) of synthesized samples $Ba_{0.86-x}La_xSn_{1.14}F_{4+x}$ and $Ba_{0.8-x}La_xSn_{1.2}F_{4+x}$ (x= 0.12) demonstrates that with an increase in the lanthanum content to 0.12 in the $Ba_{0.86-x}La_xSn_{1.14}F_{4+x}$ solid solution and to 0.10 in $Ba_{0.8-x}La_xSn_{1.2}F_{4+x}$ the conductivity increases. Substitution of a part of Ba^{2+} cations with La^{3+} cations in nodal positions probably contributes to the formation of additional interstitial anions F^-. Using the Kröger-Vink notation, this process can be represented by the following formula:

$$LaF_3\left(BaF_2\right) \rightarrow La^*_{Ba} + F_i^{'}$$

The synthesized solid solutions have a lower ionic conduction activation energy than the initial $Ba_{0.86}Sn_{1.14}F_{4.00}$ and $Ba_{0.8}Sn_{1.2}F_{4.00}$ phases, and the conduction activation energy is the lower the greater the amount of substituent in their composition. This pattern exists at both high and low temperatures (Table 1).

The presence of two straight sections on the conduction graph with different activation energy, the so-called "Faraday phase transition", indicates a change in the ionic conduction mechanism due to energetically activated structural changes in the solid electrolyte matrix [28, 31]. As a result, in the region of high temperatures, the number of additional paths for the migration of mobile F^- anions between localization sites in nodes and vacancies increases. In the conductive phases with the tetragonal structure of the fluorite derivative $PbSnF_4$, fluorine anions occupy three different positions [19, 32], differing from each other in the cationic surroundings and bond lengths, F1 - low-mobility, F2 - locally mobile, F3 – highly mobile [4, 33]. With increasing temperature, the fluorine anions of the M–F bond acquire energy sufficient to overcome the energy barrier of the transition to the interstitial space; therefore, with an increase in migration paths, the number of charge carriers also increases [32]. With a further increase in temperature, the concentration of charge carriers remains practically unchanged, but only their mobility increases. The described model of the conduction mechanism is characteristic of the obtained materials with a structure of the $MSnF_4$ type, especially in systems where the substituent has a smaller ionic radius, as well as in cases where deviation from stoichiometry promotes an increase in ionic conduction. This is confirmed by typical dependencies of conductivity on the composition, as well as by the characteristic change in conductivity and activation energy values depending on the substituent content. In the low-temperature region, conductivity is due to the migration of highly mobile fluorine ions in the planes of the interstitial space or/and the

Table 1. Conductivity parameters of solid solutions $Ba_{0.86-x}La_xSn_{1.14}F_{4+x}$ and $Ba_{0.8-x}La_xSn_{1.2}F_{4+x}$

Phase composition	ΔT, K	ΔE_a, eV ± 0,01	lg(A), (S/cm)·K	σ, S/cm ± 4%	R	T, K ± 2K
$Ba_{0.86}Sn_{1.14}F_{4.00}$	623–397	0.117	0.85	$1.34\cdot10^{-3}$	0.99	623
	397–288	0.076	0.33	$3.52\cdot10^{-4}$	1.00	288
$Ba_{0.85}La_{0.01}Sn_{1.14}F_{4.01}$	623–438	0.139	1.71	$6.39\cdot10^{-3}$	0.99	623
	438–287	0.074	0.98	$1.74\cdot10^{-3}$	0.99	287
$Ba_{0.83}La_{0.03}Sn_{1.14}F_{4.03}$	624–441	0.136	1.71	$6.60\cdot10^{-3}$	0.98	624
	441–288	0.069	0.96	$2.11\cdot10^{-3}$	0.99	288
$Ba_{0.81}La_{0.05}Sn_{1.14}F_{4.05}$	623–483	0.104	1.19	$3.57\cdot10^{-3}$	0.99	623
	483–285	0.054	0.68	$1.97\cdot10^{-3}$	1.00	285
$Ba_{0.79}La_{0.07}Sn_{1.14}F_{4.07}$	623–463	0.082	1.07	$4.06\cdot10^{-3}$	1.00	623
	463–288	0.045	0.65	$2.63\cdot10^{-3}$	1.00	288
$Ba_{0.76}La_{0.10}Sn_{1.14}F_{4.10}$	623–464	0.127	1.61	$6.13\cdot10^{-3}$	1.00	623
	464–288	0.057	0.68	$2.50\cdot10^{-3}$	0.98	288
$Ba_{0.74}La_{0.12}Sn_{1.14}F_{4.12}$	623–482	0.091	1.22	$4.88\cdot10^{-3}$	0.99	623
	482–286	0.052	0.83	$2.91\cdot10^{-3}$	1.00	286
$Ba_{0.80}Sn_{1.20}F_{4.00}$	623–455	0.092	1.06	$3.37\cdot10^{-3}$	0.98	623
	455–286	0.053	0.64	$1.79\cdot10^{-3}$	0.99	286
$Ba_{0.79}La_{0.01}Sn_{1.20}F_{4.01}$	623–487	0.129	1.50	$4.61\cdot10^{-3}$	1.00	623
	487–285	0.077	0.98	$1.56\cdot10^{-3}$	1.00	285
$Ba_{0.77}La_{0.03}Sn_{1.20}F_{4.03}$	624–455	0.105	1.29	$4.43\cdot10^{-3}$	1.00	624
	455–289	0.062	0.84	$2.03\cdot10^{-3}$	1.00	289
$Ba_{0.75}La_{0.05}Sn_{1.20}F_{4.05}$	625–434	0.098	1.26	$4.71\cdot10^{-3}$	1.00	625
	434–282	0.052	0.71	$2.27\cdot10^{-3}$	0.98	282
$Ba_{0.73}La_{0.07}Sn_{1.20}F_{4.07}$	623–502	0.194	2.16	$6.28\cdot10^{-3}$	0.99	623
	502–283	0.057	0.82	$2.37\cdot10^{-3}$	1.00	283
$Ba_{0.70}La_{0.10}Sn_{1.20}F_{4.10}$	623–474	0.090	1.32	$6.25\cdot10^{-3}$	1.00	623
	474–285	0.043	0.83	$4.13\cdot10^{-3}$	0.99	285
$Ba_{0.68}La_{0.12}Sn_{1.20}F_{4.12}$	623–507	0.141	1.72	$6.11\cdot10^{-3}$	0.99	623
	507–286	0.046	0.79	$3.36\cdot10^{-3}$	1.00	286

jumping of locally mobile fluorine ions between sites due to vacancies. In the high-temperature range, low-mobility and immobile fluoride ions can become highly mobile as a result of structurally induced changes, which allows them to effectively migrate through the sites of the crystal lattice.

It can be concluded that the obtained materials have higher conductivity than the initial compounds ($2\cdot10^{-11}$ at 333K for BaF_2 and $5\cdot10^{-7}$ at 293K for α-SnF_2 [34]) and have competitive ionic conductivity parameters compared to known highly conductive complex fluorides ($1.2\cdot10^{-3}$ at 293 K for ß-$PbSnF_4$ [4] and $1\cdot10^{-5}$ at 293 K for $BaSnF_4$ [35]). The resulting phases have also low ionic conductivity activation energy parameters compared to the most popular materials: for example, α-$PbSnF_4$ has has E_a=0.45 eV [34] at room temperature, whereas the obtained $Ba_{0.74}La_{0.12}Sn_{1.14}F_{4.12}$ and $Ba_{0.70}La_{0.10}Sn_{1.20}F_{4.10}$ show E_a~0.05 eV at room temperature.

The obtained results on the electrical conductivity of non-stoichiometric phases in the BaF_2–LaF_3–SnF_2 system [35, 36] made it possible to construct an isothermal surface of the electrical conductivity of fluorine-conducting phases $Ba_{1-y-x}La_xSn_{1+y}F_{4+x}$ depending on the content of substituents. Fig. 5 shows that the electrical conductivity increases with an increase in the concentration of lanthanum and tin in their composition.

An important requirement for solid fluoride electrolytes used in fluoride-ion batteries is low electron conductivity. Therefore, the dependences of the electron conductiv-

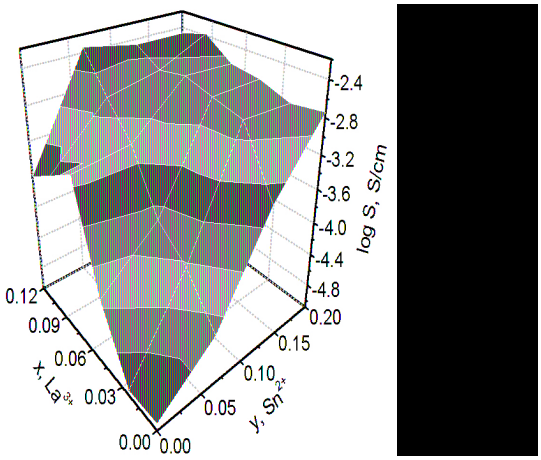

Fig. 5. Isothermal conductivity surface of solid solutions $Ba_{1-y-x}La_xSn_{1+y}F_{4+x}$ at RT depending on composition.

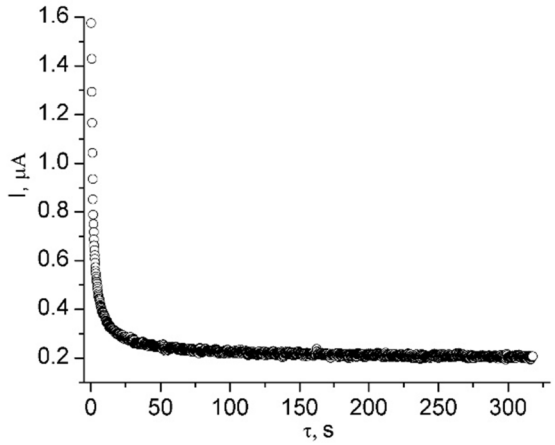

Fig. 6. Dependence of the current flowing through the cell $Ni:NiF_2:CaF_2|Ba_{0.80}La_{0.10}SnF_{4.10}|Pt$, on the polarization time (E = 1.6 B) at 473 K.

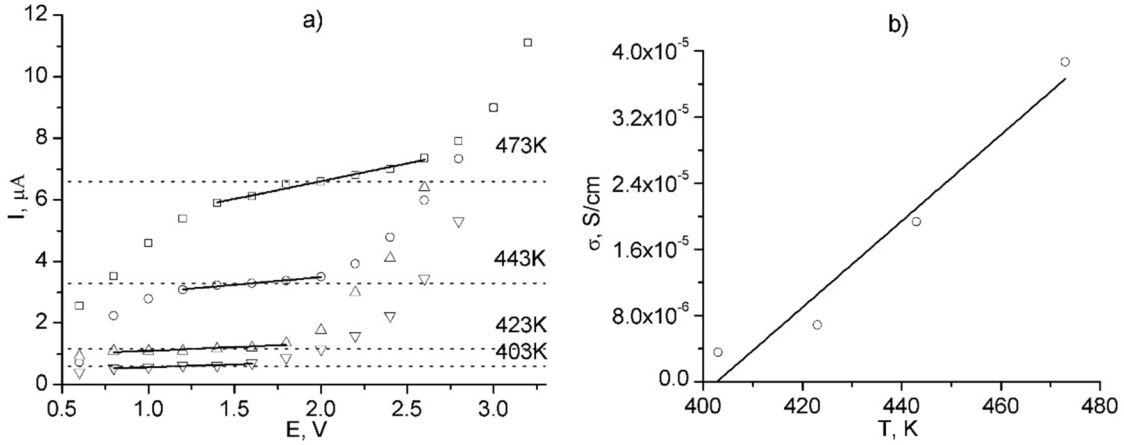

Fig.7. Region of stationary current values at volt-ampere characteristics (a) and electron conductivity at different temperatures (б) for the $Ba_{0.80}La_{0.10}Sn_{1.10}F_{4.10}$ fluorine-conducting phase

ity on the content of lanthanum, tin and temperature were investigated. Electron conductivity was determined by the Hebb-Wagner method by analyzing the voltage-current dependencies of the electrochemical cell $Ni:NiF_2:CaF_2|electrolyte|Pt$. If a constant voltage is applied to this system, will move in the electric field from the cathode to the anode, where they accumulate. This process leads to a drop in current on the voltammogram; and upon reaching a certain value of the concentration of electrons and/or holes in the solid electrolyte, the current reaches a minimum steady-state value (Fig. 6). The time to achieve a steady state can range from a few minutes to several hours. This effect is described by the equation:

$$I_s = I_n + I_p = \left(\sigma_n\left[1-\exp\left(-\frac{EF}{RT}\right)\right]+\sigma_p\left[\exp\left(\frac{EF}{RT}-1\right)\right]\right)\frac{RTS}{Fl} \quad (2)$$

where σ_n and σ_p are the specific conductivity of electrons and holes, respectively; E is the applied voltage; T is the temperature; R is the universal gas constant; S is the contact area, F is the Faraday constant, l is the electrolyte thickness [29].

If the cell is significantly dominated by n-type electron conductivity ($\sigma_n > \sigma_p$), the equation (3) can be simplified and represented as follows:

$$I_s = \frac{RTS\sigma_n}{Fl}\left(1-\exp\left(-\frac{EF}{RT}\right)\right) \quad (3)$$

From this equation it follows that that the current $I_s = f(E)$ takes on stationary values at certain voltage values (Fig. 7,8,9).

For the region of stationary current values, the condition $EF>>RT$ is satisfied, so the expression can be represented as equation (4). From this equation, σ_n was determined, then

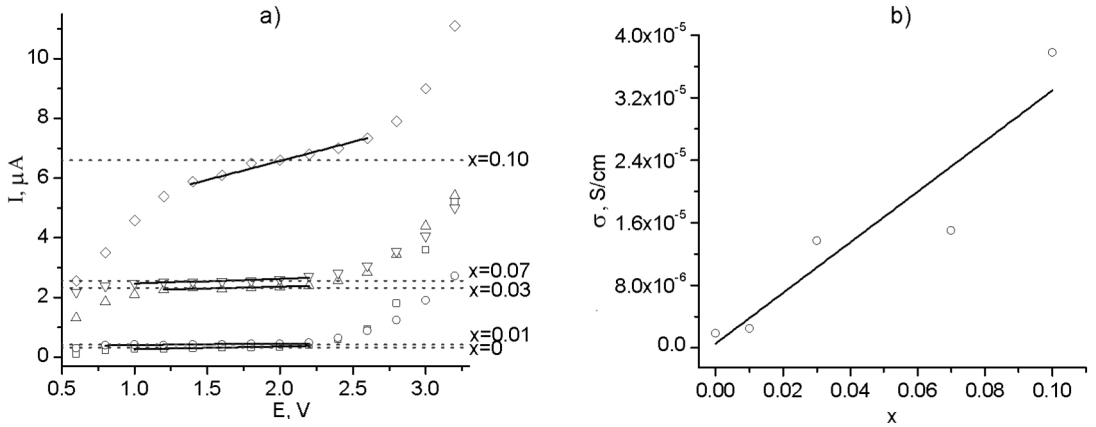

Fig.8. The region of stationary current values (a) on volt-ampere characteristics and electron conductivity at different concentrations (x, mole fractions) of lanthanum (b) for fluorine-conducting phases of the composition $Ba_{0.9-x}La_xSn_{1.1}F_{4+x}$.

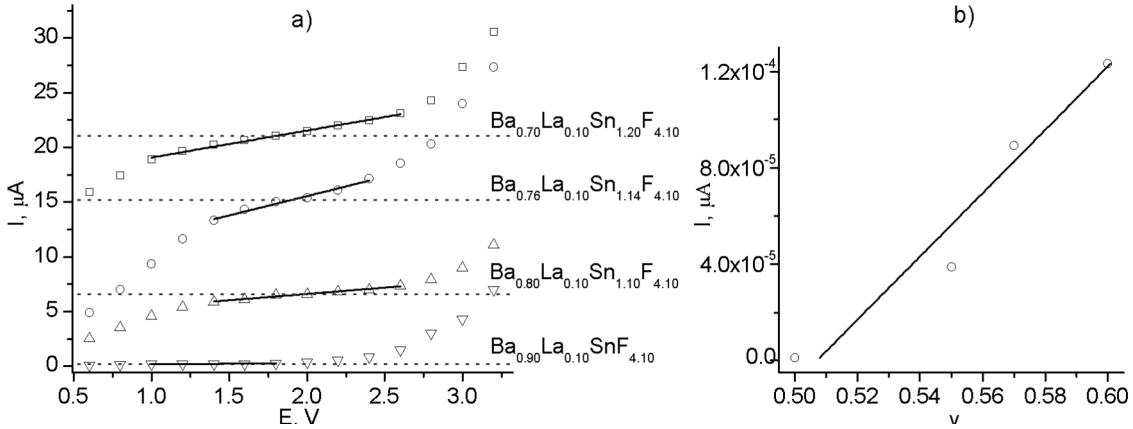

Fig.9. The region of stationary current values (a) at volt-ampere characteristics and electron conductivity at different concentrations (y, mole fractions) of tin in solid solution $Ba_{1-y-x}La_xSn_{1+y}F_{4+x}$ x=0.10, y≤0.2 (b).

the charge transfer numbers of fluorine anions were estimated using equation (5).

$$I_s = \frac{RTS\sigma_n}{Fl}; \quad (4)$$

$$t_{F^-} = 1 - \frac{\sigma_n}{\sigma}. \quad (5)$$

Fig. 7a shows the typical nature of the dependence of electron conductivity on composition and temperature using the example of the fluorine-conducting phase $Ba_{0.80}La_{0.10}Sn_{1.10}F_{4.10}$. Based on the obtained data, the electronic component of conductivity was estimated (Table 2). It was found that it increases proportionally with increasing temperature (Fig. 7b) and is significantly lower than the total conductivity.

It was found that in the $Ba_{0.9-x}La_xSn_{1.1}F_{4+x}$ phases, an increase in the concentration of lanthanum causes an increase in electron conductivity (Fig. 8b); however, judging by the calculated charge transfer numbers (Table 2), this does not have a significant effect on the total conductivity, which indicates that charge transfer is provided exclusively by fluorine anions.

In phases with a lanthanum content of 0.10, the dependence of the electronic component of conductivity on the concentration of tin cations (Fig. 9a) is linear and increases with increasing tin content (Fig. 9b). The sample $Ba_{0.70}La_{0.10}Sn_{1.20}F_{4.10}$ with the highest tin content has the highest electron conductivity. Charge transfer numbers range from 0.95 to 1.00 in these phases (Table 2). However, even in this case, the synthesized phases have unipolar conductivity, which is provided by fluorine anions.

The charge transfer numbers calculated from Hebb-Wagner polarization data are practically independent of the quantitative and qualitative composition of the synthesized phases and are close to 1. This suggests that charge transfer in the synthesized phases is provided exclusively by fluorine anions.

Table 2. Electron conductivity of non-stoichiometric phases of $Ba_{1-y-x}La_xSn_{1+y}F_{4+x}$ composition.

Sample	I_s, μA	$\sigma_{n\ electron}$, S/cm	t_{F^-}	T, K	$\sigma_{n\ total}$ S/cm
$Ba_{0.80}La_{0.10}Sn_{1.10}F_{4.10}$	0.61	$3.52\cdot10^{-6}$	1.00	403	$2.44\cdot10^{-3}$
$Ba_{0.80}La_{0.10}Sn_{1.10}F_{4.10}$	1.16	$6.80\cdot10^{-6}$	1.00	423	$2.49\cdot10^{-3}$
$Ba_{0.80}La_{0.10}Sn_{1.10}F_{4.10}$	3.29	$1.93\cdot10^{-5}$	0.99	453	$2.66\cdot10^{-3}$
$Ba_{0.80}La_{0.10}Sn_{1.10}F_{4.10}$	6.60	$3.87\cdot10^{-5}$	0.99	473	$2.78\cdot10^{-3}$
$Ba_{0.83}La_{0.07}Sn_{1.10}F_{4.07}$	2.56	$1.50\cdot10^{-5}$	0.99	473	$1.94\cdot10^{-3}$
$Ba_{0.87}La_{0.03}Sn_{1.10}F_{4.03}$	2.33	$1.37\cdot10^{-5}$	0.97	473	$4.60\cdot10^{-4}$
$Ba_{0.89}La_{0.01}Sn_{1.10}F_{4.01}$	0.43	$2.50\cdot10^{-6}$	0.99	473	$3.51\cdot10^{-4}$
$Ba_{0.90}Sn_{1.10}F_4$	0.32	$1.88\cdot10^{-6}$	0.99	473	$3.24\cdot10^{-4}$
$Ba_{0.90}La_{0.10}SnF_{4.10}$	0.20	$1.17\cdot10^{-6}$	1.00	473	$9.95\cdot10^{-4}$
$Ba_{0.76}La_{0.10}Sn_{1.14}F_{4.10}$	15.21	$8.91\cdot10^{-5}$	0.98	473	$3.99\cdot10^{-3}$
$Ba_{0.70}La_{0.10}Sn_{1.20}F_{4.10}$	21.06	$1.23\cdot10^{-4}$	0.95	473	$2.61\cdot10^{-3}$

Taking into account the obtained results, the studied phases can be considered promising materials for use as solid fluorine-ion electrolytes in various electrochemical devices. The obtained materials meet the key requirements for modern solid electrolytes and demonstrate competitive values of ionic conductivity, activation energy, electronic conductivity, compared to known fluorine conductors based on BaF_2, LaF_3, or $PbSnF_4$. In addition, the proposed synthesis method is technologically available.

4. Conclusions

It was found that non-stoichiometric $Ba_{0.86-x}La_xSn_{1.14}F_{4+x}$ and $Ba_{0.8-x}La_xSn_{1.2}F_{4+x}$ ($x < 0.12$) phases with a tetragonal crystal lattice can be obtained by sintering solid solutions $Ba_{1-x}La_xF_{2+x}$ ($x < 0.12$) with tin (II) fluoride.

The substitution of some of barium cations in the initial phases of $Ba_{0.86}Sn_{1.1}F_{4.00}$ and $Ba_{0.80}Sn_{1.20}F_{4.00}$ with lanthanum cations promotes an increase in conductivity to a greater extent, the higher the concentration of the substituent. The highest conductivity is observed in samples of the composition $Ba_{0.74}La_{0.12}Sn_{1.14}F_{4.12}$ ($2.91\cdot10^{-3}$ S/cm at RT) and the $Ba_{0.70}La_{0.10}Sn_{1.20}F_{4.10}$ ($4.13\cdot10^{-3}$ S/cm at RT). The activation energy of the conductivity of the fluorine-conducting phases of this composition is lower than the activation energy of the initial phases.

Analysis of the isothermal surface of conductivity of fluorine-conducting phases $Ba_{1-y-x}La_xSn_{1+y}F_{4+x}$ demostrates an increase in the ionic conductivity with increasing content of the substituent in the studied concentration ranges ($0 \le x \le 0.12$ for lanthanum), ($0 \le y \le 0.20$ for tin).

It was found that the pressure under which samples are prepared for conductivity studies affects both their density and conductivity. With increasing pressure, the density of synthesized samples of fluorine-conducting phases increases exponentially. The curve of the dependence of conductivity on pressure during the preparation of samples of synthesized phases has an extremum. With increasing pressure, conductivity first increases, and after reaching the limit values it decreases. This may be associated with structural and mechanical transformations of crystallites at both the micron and submicron and atomic-molecular levels. When pressure only results in a reduction in crystallite size (compaction) at the micron and submicron levels, this contributes to an increase in conductivity, and when pressure results in deformation of the crystal lattice, this leads to a decrease in conductivity.

References

1. V. Kumaravel, J. Bartlett, S.C. Pillai, 2020. Solid electrolytes for high-temperature stable batteries and supercapacitors. Adv Energy Mater. 11 (3), 2002869. https://doi: 10.1002/aenm.202002869.
2. A. Xiao, G. Galatolo, M. Pasta, The case for fluoride-ion batteries, Joule, 5(11) (2021) 2823-2844. https://doi.org/10.1016/j.joule.2021.09.016
3. F. Gschwind, G. Rodriguez-Garcia, D.J.S. Sandbeck et. al., Fluoride ion batteries: Theoretical performance, safety, toxicity, and a combinatorial screening of new electrodes, J. Fluor. Chem., 182 (2016) 76-90. https://doi.org/10.1016/j.jfluchem.2015.12.002
4. M.A. Nowroozi, I. Mohammad, P. Molaiyan, et. al., Fluoride ion batteries – past, present, and future, J Mater Chem A., 9 (2021) 5980-6012. https://doi: 10.1039/d0ta11656d.
5. S. Gopinadh, P. Phanendra, B.John et. al., 2022. Fluoride-ion batteries: State-of-the-art and future perspectives. SM&T, 32, e00436. https://doi.org/10.1016/j.susmat.2022.e00436.

6. T. Liu, N. Peng, X. Zhang, et al., Insight into anion storage batteries: Materials, properties and challenges, Energy Stor. Mater., 42 (2021) 42-67. https://doi.org/10.1016/j.ensm.2021.07.011.
7. M. Zhang , X. Cao, Y. Hao et. al., 2024. Recent progress, challenges and prospects of electrolytes for fluoride-ion batteries. Energy Reviews. 3(3), 100083. https://doi.org/10.1016/j.enrev.2024.100083
8. J. Wang, J. Hao, C. Duan, et. al., 2021. A Fluoride-Ion-Conducting Solid Electrolyte with Both High Conductivity and Excellent Electrochemical Stability. Small., 18(5), 2104508. https://doi.org/10.1002/smll.202104508
9. S. Vilminot, G. Perez, W. Granier, et. al., High ionic conductivity in new fluorine compounds of tin II. I. On $PbSnF_4$: Relation between structure and conductivity, Solid State Ion., 2(2) (1981), 87-90. https://doi.org/10.1016/0167-2738(81)90003-5
10. R. Kanno, S. Nakamura, K. Ohno, et. al., Ionic conductivity of tetragonal $PbSnF_4$ prepared by solid state reaction in HF atmosphere, Mat. Res. Bull., 26(11) (1991) 1111-1117. https://doi.org/10.1016/0025-5408(91)90116-4
11. F. Gschwind, J. Bastien, Parametric investigation of room-temperature fluoride-ion batteries: assessment of electrolytes, Mg-based anodes, and BiF_3-cathodes, J. Mater. Chem. A., 3 (2015) 5628-5634. https://doi.org/10.1039/C4TA06625A
12. D. McTaggart, S. Warren, O. Clemens, 2023. Reconsidering Anode Materials for Fluoride-Ion Batteries–The Unexpected Roles of Carbide Formation. ChemSusChem., 16(18), e202300486. https://doi.org/10.1002/cssc.202300486
13. K. Mori, A. Mineshige, T. Emoto et al., Electrochemical, thermal, and structural features of BaF_2–SnF_2 fluoride-ion electrolytes, J Phys Chem C. 125 (2021). 12568-12577. https://doi: 10.1021/acs.jpcc.1c03326.
14. L. Liu, L. Yang, M. Liu, et. al., 2020. SnF_2-based fluoride ion electrolytes $MSnF_4$ (M = Ba, Pb) for the application of room-temperature solid-state fluoride ion batteries. J. Alloys Compd., 819, 152983. https://doi.org/10.1016/j.jallcom.2019.152983
15. G. Dénès, A. Muntasar, A. Madamba, et. al., The unique case of tin(II) fluoride containing unexpected substitutional solid solutions: local structure versus global structure, WIT Transactions on Engineering Sciences. 116 (2017) 223-234. https://doi.org/10.2495/MC170231.
16. L.N. Patro, K. Hariharan, Fast fluoride ion conducting materials in solid state ionics: an overview, Solid State Ionics. 239 (2013) 41-49. https://doi: 10.1016/j.ssi.2013.03.009.
17. S. Chaudhuri, F. Wang, C.P. Grey, Resolving the different dynamics of the fluorine sublattices in the anionic conductor BaSnF4 by using high-resolution MAS NMR techniques, J Am Chem Soc. 124 (2002) 11746-11757. https://doi: 10.1021/ja026155j.
18. L.N. Patro, K. Hariharan, Rare earth ions (Eu^{3+} and Nd^{3+}) doped $BaSnF_4$: transport and photoluminescence characteristics, Ionics. 19 (2013) 1611-1617. https://doi: 10.1007/s11581-013-0896-z.
19. L. Liu, L. Yang, D. Shao, et. al., Nd3+ doped $BaSnF_4$ solid electrolyte for advanced room temperature solid-state fluoride ion batteries, Ceram Int. 46 (2020) 20521-20528. https://doi: 10.1016/j.ceramint.2020.05.16.
20. R. Pshenychnyi, O. Lysenko, T. Pavlenko, et. al., Conductive properties of solid solutions of the system xYF_{3}-$_{(1-x)}BaF_2$-SnF_2, Funct Mater. 30 (2023) 18-23. https://doi: 10.15407/fm30.01.18.
21. T. Shen, S. Li, K. Yue, et. al., LiF doped ß-PbSnF4 with improved ionic conductivity toward high-performance all-solid-state fluoride-ion batteries, J. Mater. Chem. A. 13 (2025) 14995-15001. https://doi.org/10.1039/D5TA01188D
22. Z. Zang, L. Liu, L. Yang, et. al., Preparation and Performance of Eu^{3+}-Doped $BaSnF_4$-Based Solid-State Electrolytes for Room-Temperature Fluoride-Ion Batteries, ACS Sustainable Chem. Eng. 9(38) (2021) 12978-12989. https://doi.org/10.1021/acssuschemeng.1c04523
23. J. Liu, L. Yi, P. Zeng, et al., Point defect engineering enabled the high ionic conductivity of $BaSnF_4$ for solid-state fluoride-ion batteries at room temperature, Energy Fuels. 36(24) (2022) 15258–15267. https://doi: 10.1021/acs.energyfuels.2c03509.
24. R. Pshenychnyi, T. Pavlenko, Yu. Pohorenko, et al., Synthesis, structure and properties of solid solutions $Ba_{1-x}Sn_{1+x}F_4$ and $(K_yBa_{1-y})_{(1-x)}Sn_{1+x}F_{4-y(1-x)}$, Voprosy Khimii i Khimicheskoi Tekhnologii. 1 (2021) 62-70. https://doi: 10.32434/0321-4095-2021-134-1-62-70.
25. H. Chen, T. Aalto, V. Vanita, et. al., 2024. Effect of Uniaxial Stack Pressure on the Performance of Nanocrystalline Electrolytes and Electrode Composites for All-Solid-State Fluoride-Ion Batteries. Small Structures, 5(7), 2300570. https://doi.org/10.1002/sstr.202300570
26. C. Schneider, C.P. Schmidt, A. Neumann, et. al., 2023. Effect of Particle Size and Pressure on the Transport Properties of the Fast Ion Conductor *t*-Li_7SiPS_8. Adv. Energy Mater., 13(5), 2203873. https://doi.org/10.1002/aenm.202203873

27. Yu. Pogorenko, R. Pshenychnyi, V. Lutsyk, et. al., 2017. Transport Properties of Aliovalent Substitution Solid Solutions of the System (1-x)$PbF_{2-x}YF_3$-SnF_2. IOP Conf. Ser.: Mater. Sci. Eng. 175, 012039. https://doi10.1088/1757-899X/175/1/012039
28. Yu. Pogorenko, R. Pshenychnyi, A. Omelchuk, V. Trachevskyi, Conductivity of aliovalent substitution solid solutions $Pb_{1-x}R_xSnF_{4+x}$, Solid State Ionics. 338 (2019) 80-86. https://doi:10.1016/j.ssi.2019.05.001.
29. J. Wagner, C. Wagner Electrical conductivity measurements on cuprous halides, J Chem Phys. 26 (1957) 1597-1601. https://doi:10.1063/1.1743590.
30. R. Shannon, Revised effective ionic radii and systematic studies of interatomic distances in halides and chalcogenides, Acta Cryst A. 32 (1976) 751-767. https://doi:10.1107/S0567739476001551.
31. Sh. Yoshikado, Y. Ito, J.M. Réau, Fluoride ion conduction in $Pb_{1-x}Sn_xF_2$ solid solution system, Solid State Ionics. 154-155 (2002) 503-509. https://doi.org/10.1016/S0167-2738(02)00489-7
32. Y. Pogorenko, R. Pshenychnyi, A. Omelchuk et. al., Synthesis and conductivity properties of solid solutions $Pb_{1-x}Ln_xSnF_{4+x}$ (Ln — La, Ce, Nd, Sm, Gd), Ukr. Chem. J.. 3(82) (2016) 33-43. ISSN 0041-6045.
33. Y. Ito, T. Mukoyama, H. Funatomi, et. al., The crystal structure of tetragonal form $PbSnF_4$, Solid State Ionics. 67(3-4) (1994) 301-305. https://doi.org/10.1016/0167-2738(94)90021-3
34. M. A. Reddy, M. Fichtner Fluoride-Ion Conductors, in: N.J. Dudney, W.C. West, J. Nanda (Eds.) Materials and Energy: Volume 6 Handbook of Solid State Batteries 2nd Edition, World Scientific, Singapore, 2015, p. 277-306.
35. O. Lysenko, R. Pshenychnyi, T. Pavlenko, et. al., Synthesis, structure and electrophysical properties of fluoride-conducting phases $Ba_{1-x}La_xSnF_{4+x}$, Chem. Chem. Technol. 18(3) (2024) 313-320. https://doi: 10.23939/chcht18.03.313
36. O. Lysenko, R. Pshenychnyi, A. Omelchuk, Conductivity of non-stoichiometric fluoride-conducting phases $Ba_{0.9-x}La_xSn_{1.1}F_{4+x}$, Voprosy Khimii i Khimicheskoi Tekhnologii. 2 (2025) 87-93. https://doi: 10.32434/0321-4095-2025-159-2-87-93